Molecular Dynamics Study of the Energetic, Mechanistic, and Structural Implications of a Closed Phosphate Tube in ncd

Todd J. Minehardt,* Roger Cooke,† Edward Pate,‡ and Peter A. Kollman*

*Department of Pharmaceutical Chemistry and †Department of Biochemistry and Biophysics and Cardiovascular Research Institute, University of California, San Francisco, California 94143, and ‡Department of Pure and Applied Mathematics, Washington State University, Pullman, Washington 99164 USA

ABSTRACT The switch 1 region of myosin forms a lid over the nucleotide phosphates as part of a structure known as the phosphate-tube. The homologous region in kinesin-family motors is more open, not interacting with the nucleotide. We used molecular dynamics (MD) simulations to examine a possible displacement of switch 1 of the microtubule motor, ncd, from the open conformation to the closed conformation seen in myosin. MD simulations were done of both the open and the closed conformations, with either MgADP or MgATP at the active site. All MD structures were stable at 300 K for 500 ps, implying that the open and closed conformers all represented local minima on a global free energy surface. Free energy calculations indicated that the open structure was energetically favored with MgADP at the active site, suggesting why only the open structure has been captured in crystallographic work. With MgATP, the closed and open structures had roughly equal energies. Simulated annealing MD showed the transformation from the closed phosphate-tube ncd structure to an open configuration. The MD simulations also showed that the coordination of switch 1 to the nucleotide dramatically affected the position of both the bound nucleotide and switch 2 and that a closed phosphate-tube may be necessary for catalysis.

INTRODUCTION

The mechanism by which motor proteins and the triphosphate substrate interact to produce force and motion remains a fundamental and unresolved question in biophysics. The recent x-ray crystallographic structures of proteolytically or genetically truncated myosin (both to be termed S1), with and without bound nucleotide (Smith and Rayment, 1996a; Fisher et al., 1995; Gulick et al., 1997, 2000; Dominguez et al., 1998; Houdusse et al., 1999), the motor domains of the monomeric microtubule (MT) motors ncd, kinesin, and Kar3 (Kull et al., 1996; Sablin et al., 1996; Gulick et al., 1998), and the kinesin and ncd dimers (Kozielski et al., 1997; Sablin et al., 1998; Müller et al., 1999) have all brought renewed stimulus to efforts to resolve this question. The most surprising revelation from these crystal structures was the obvious and significant structural homology that exists among the kinesin-family, MT motors, and the core of S1, suggesting that common chemomechanical mechanisms may exist (reviewed in Kull et al., 1996, 1998; Gulick et al., 1998; Vale, 1996; Sack et al., 1999).

The nucleotide-binding site is contained within the structurally homologous region of these proteins. The triphosphate-binding portion of the nucleotide site in both classes of motors is composed of three structural elements with universally conserved amino acid (aa) sequences. The first is the P-loop, containing the Walker A motif (Walker et al., 1982) with conserved aa sequence Gx_4GKT/S and corresponding to aa 179–186 in *Dictyostelium discoideum* (Dd) myosin and 434–441 in *Drosophila melanogaster* (Dm) ncd. The second is switch 1, containing conserved aa sequence NxxSSR and corresponding to aa 233–238 in Dd myosin and 544–549 in Dm ncd. The third structural element is switch 2, containing conserved aa sequence DxxGxE and corresponding to aa 454–459 in Dd myosin and aa 580–585 in Dm ncd.

Despite the sequence homology, there is a significant difference in the structural topologies in the triphosphate binding regions. In S1, the P-loop, switch 1, and switch 2 together form a narrow tunnel referred to as the phosphate-tube (P_i-tube) in which a bound di- or triphosphate or analog resides (Yount et al., 1995). Extensive protein-metal-phosphate interactions are evident from the crystal structures. In the kinesin-family motor structures, however, the switch 1 region has a very different structure and does not form a P_i-tube. Structural overlays of the triphosphate-binding domains of S1 and kinesin-family motors show a displacement of switch 1 away from the nucleotide phosphates, opening what would be the P_i-tube in S1 (see Fig. 1 *A*).

The open binding pocket in the kinesin-family motor structures more closely resembles a solvent-exposed trough in which the nucleotide (ADP) rests (Fig. 1 *A*). Only limited interaction between the nucleotide and the protein is observed. Indeed, one can seriously question whether such an open structure could sufficiently control the transition nucleotide state and its relationship to the catalytic water to allow hydrolysis to proceed at the experimentally observed, microtubule-activated rate of 20 s^{-1} at 20°C in kinesin (Ma and Taylor, 1997). We have previously shown that the closed P_i-tube in myosin crystal structures must undergo a

Received for publication 14 August 2000 and in final form 20 November 2000.

T. J. Minehardt's present address: Department of Chemistry, Princeton University, Princeton, NJ 08544.

Address reprint requests to Dr. Peter A. Kollman, Department of Pharmaceutical Chemistry, School of Pharmacy, University of California, 513 Parnassus Avenue, Suite S 92, San Francisco, CA 94143. Tel.: 415-476-4637; Fax: 415-502-1411; E-mail: pak@cgl.ucsf.edu.

0006-3495/01/03/1151/18 $2.00

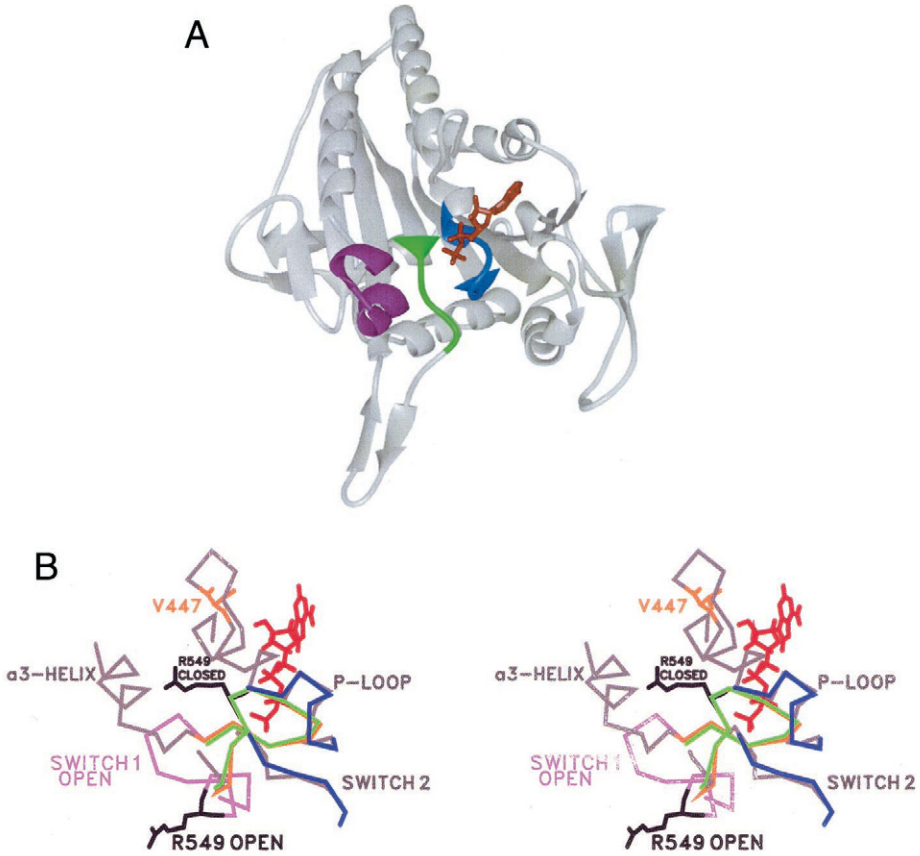

FIGURE 1 (*A*) Ribbon diagram of the Dm ncd structure. ADP is in red. The three regions comprising the nucleotide phosphate binding domain, the P-loop (blue), switch 2 (green), and the switch 1 region (magenta) are shown. Switch 2 is displaced away from the nucleotide. (*B*) Stereo pair overlay of the nucleotide-binding region of Dm ncd and Dd S1 (C_α backbone). The ncd crystal structure is in gray, except for the switch 1 region, which is in magenta. The P-loop and switch 2 of S1 are in dark blue. Structures were superimposed at the P-loops. Switch 1 is pulled back from the nucleotide in the ncd structure (also see magenta region of *A*). The switch 1 region of S1 (orange) instead projects over the nucleotide. Green shows the modeled switch 1 region of ncd, using the corresponding orange region of S1 as a template. In ncd, the magenta-to-green transition closes the P_i-tube. Arg 549 is shown in black in both the open and closed conformations for reference. The displacement in the transition is 11 Å (C_α—C_α). The side chain of Val 447 protruding from a β-hairpin is shown in orange.

significant opening during its motor cycle (Pate et al., 1997). This was accomplished by experimentally showing that S1, acto-S1, and actomyosin were able to bind to ATP analogs that were modified at the γ-phosphorus (P_γ) position with moieties that were too large to fit through the closed P_i-tube observed in the crystal structures. When bound, these analogs functioned as classical, competitive inhibitors. Others have shown similar binding of P_γ-modified analogs (Sleep et al., 1994). Amino acid sequence conservation between proteins is frequently observed to imply functional similarity as well. Thus we consider the question of whether the open P_i-tube in the kinesin-family motor structures can close during the hydrolysis cycle. The existence of such a state could also potentially circumvent any catalytic problems outlined above.

A number of other lines of evidence support the hypothesis of movements in the switch 1 region in kinesin-family motors. The term switch 1 is frequently restricted to the universally conserved NxxSSR sequence in motor proteins. In the kinesin-family motors, this is part of a loop–α-helix (L9, α3a) motif, bordered on the N-terminus end by the β5-ribbon that forms part of the core, eight-stranded, β-sheet platform of the kinesin-family motors, and on the C-terminus end by the α3-helix, which forms one lip of the nucleotide-binding site (Kull et al., 1996; Sablin et al., 1996; Gulick et al., 1998; Kozielski et al., 1997; Müller et al., 1999). To fix terminology, we will use the term switch 1 region to include the extended region of residues between α3 and β5 (aa 542–553 in ncd, 193–204 in kinesin, and 588–599 in Kar3). A comparison of the switch 1 regions in Kar3, ncd, and kinesin monomeric crystal structures, respectively, shows a progressive displacement of the switch 1 region away from the nucleotide. The distances from the P_β of ADP to the point at which the switch 1 region loop, L9, enters the α3-helix (all to C_α of aa 586 in Kar3, 539 in ncd, and 191 in kinesin) are 8.8 Å, 13.1 Å, and 17.3 Å, respectively. Thus, crystal structure data themselves imply the possibility of significant movement in the switch 1 region. Kinesin-family motors, actin-based motors, and the G-proteins are homologous members of a super-family deriving from a common ancestor (Kull et al., 1998). Observations of switch 1 displacements away from the nucleotide in G-proteins (Pai et al., 1990; Tong et al., 1991; Kjeldgaard et al., 1993; Goldberg, 1999) provide further support for the possibility of similar movements in the switch 1 region of kinesin-family motors. This movement has also been implicated as crucial for nucleotide exchange to occur in G-proteins.

More recently, we have compared the switch 1 regions in ncd and myosin and used graphical visualization tools to close the P_i-tube of ncd (Pate, 1999). In S1, switch 1 is a loop that extends over the triphosphates, forming one side of

the closed Pi-tube (Fig. 1, *A* and *B*). In our model, the α-helix–loop motif in the switch 1 region of ncd was modified using switch 1 of the Dd S1·ADP·BeFx structure (Fisher et al., 1995) as a template. The ncd structure formed from superposition of this switch-1-modified ncd showed a structure analogous to the closed P_i-tube in the S1 structure. It furthermore appeared that much of the coordination between switch 1 and the triphosphates identified in the S1 structure could be maintained. This provided additional structural and energetic support for the possibility of a closing of the P_i-tube in kinesin-family motors.

A serious limitation of the above graphical visualization analysis is its inherently static nature. Molecular dynamics (MD) on the other hand provides a powerful tool for investigating both the energetics and structural implications of the interaction of a substrate with a ligand in the presence of solvent and thermal fluctuations. Recently, methods have become available that allow us to more accurately determine the free energy differences of various conformers in solution (Osapay et al., 1996; Bashford et al., 1997; Demchuk et al., 1997; Yang and Honig, 1995a,b; Yang et al., 1996; Smith and Honig, 1994; Honig et al., 1993). These Poisson-Boltzmann surface area (PBSA) methods are more accurate than the generalized Born approach for more realistic treatments of complex solutes in general, and for the solvation of highly charged species in particular (Srinivasan et al., 1998; Massova and Kollman, 1999). Here we use MD to further examine the structural and energetic implications of a closing of the P_i-tube in ncd via a displacement of the switch 1 region.

METHODS

Molecular dynamics

All MD simulations were performed using the standard AMBER 5.0 suite of programs (Case et al., 1997) and the Cornell (Cornell et al., 1995) force field. We followed the same basic preparation procedure as outlined by Chong and co-workers (1999). The LEaP module of AMBER 5.0 was used to add hydrogens to the protein. Histidine residues were all protonated only at N_δ in consideration of neighboring amino acids that would interact differently with histidine residues possessing different charged states at physiological conditions. Charges for ADP and ATP were derived by first performing a single-point energy calculation at the Hartree-Fock level of theory using a 6–31G* basis set to obtain electrostatic charges. These were then fit to the molecules by using the RESP procedure (Bayly et al., 1993). An energy minimization over the entire protein-ligand complex was then done to generate the starting structures for MD calculations. For energy minimizations, we first did 10 steps using the method of steepest descent. This was followed by 990 steps of conjugate gradient minimization. Typical root mean square (rms) values for the gradient vector were on the order of 0.1 after 1000 cycles were completed.

MD simulations were performed with the switch 1 region positioned such that the P_i-tube was closed or open, and with either MgADP or MgATP at the nucleotide site. For more definite notations, these structures will be referred to as ADP-closed, ATP-open, etc. Because computational considerations precluded our simulating the entire, fully solvated system (~20,000 atoms), we instead followed the common practice of choosing a spherical region of the protein-nucleotide complex in water and allowed atoms within this area to move while holding others fixed in their minimized positions. This was termed the belly. The size of the belly was then chosen sufficiently large as to include all moieties that participated in any significant short- and long-range interactions with the nucleotide-binding domain. The positions of the P_β atoms were slightly different in the ADP and ATP structures. However, we used identical bellies of radius 16 Å specified about the same center (P_β of the crystal structure) in the two open and two closed structures. This was to ensure that subsequent energetic and structural analyses would be internally consistent. For all simulations, the LEaP module of AMBER 5.0 was used to add a solvent cap of inflexible TIP3P waters (Jorgensen et al., 1983) of radius 22 Å from the location of the β-phosphorus. This water cap was held in place by a soft half-harmonic potential (Pearlman et al., 1995). Because our simulations included explicit waters, the dielectric function was held constant; i.e., the dielectric constant of TIP3P waters was implicitly employed. Each simulation contained approximately 600 water atoms and 2000 protein and nucleotide atoms.

Each MD simulation can be described as the sum of four individual steps. In the first, we minimize only the waters within the belly using 1000 cycles of energy minimization as described above. During the second, we heat these waters to 300 K over the course of 50 ps. Another minimization is performed at the third step, in which we now allow all atoms within the belly to move. The fourth step consists of heating the entire belly to 300 K. The structure is then allowed to evolve for 500 ps. Temperature is regulated by coupling the system to an external bath and utilizes separate scaling factors for solvent and solute atoms. This reduces the formation of hot and/or cold spots as heating progresses (Berendsen et al., 1984). The long-range nonbonded interactions were limited to 14 Å using a residue-based cutoff scheme. The SHAKE algorithm (Ryckaert et al., 1977) was employed, and we used a 2-fs time step. Smaller time steps did not change our conclusions. The calculated MD trajectory was written to disk every 1 ps for subsequent data analysis.

Energy analyses

Snapshots from the MD trajectories were processed to compute the average quantities that are reported. Typically, anywhere from 5 to 25 snapshots from the last 200–300 ps of a 500-ps simulation sufficed for convergence of the desired quantities. We used 10 snapshots from the trajectories, each representing 20 ps in time, for the PBSA calculations. We note that converged quantities were seen for as few as 4 snapshots.

Of interest to us were the free energies of the open and closed conformers. We estimated the free energies from the MD trajectories as done by Srinivasan et al. (1998) and Massova and Kollman (1999):

$$\langle G \rangle = \langle E_{MM} \rangle + \langle G_{PBSA} \rangle - T\langle S_{MM} \rangle \quad (1)$$

The average free energy of the system over a series of MD snapshots (Eq. 1) is estimated to be a sum of the average molecular mechanical energy (itself a sum of the electrostatic, van der Waals, and internal energies), $\langle E_{MM} \rangle$, the sum of the average solvation nonpolar and polar (PBSA) energies, $\langle G_{PBSA} \rangle$, and the free energy due to the average entropy of the snapshots, $T\langle S_{MM} \rangle$. We employed Delphi 2.0 (Sharp and Honig, 1990) to calculate the electrostatic term (described in detail in Chong et. al., 1999; Srinivasan et. al., 1998; Massova and Kollman, 1999), and the solvent-accessible surface area (SASA) algorithm of Sanner (Sanner et al., 1996) to compute the nonpolar term. The magnitude and size of the binding free energy was very dependent upon the size we chose for the radius of the hydrated Mg^{2+} cation. We used 1.45 Å because this number has been shown to reproduce experimentally determined hydration free energies (Aqvist, 1992).

$$\Delta G = \langle G \rangle_{complex} - \langle G \rangle_{receptor} - \langle G \rangle_{ligand}. \quad (2)$$

Eq. 2 can be used to calculate the binding free energy of two molecules in a number of ways. If one runs only a simulation of the complex, one can calculate the free energy evaluating Eq. 1 for complex, receptor, and ligand

using the same snapshots. This approach assumes no conformational change upon binding. We estimate the entropy term (see Results) due to the difficulty in computing it directly. However, one can also do separate trajectories for all three species and, after using Eq. 1 to evaluate their free energies, use Eq. 2 to calculate an estimated binding free energy.

Analysis and comparison of structures

Except as noted, all MD and x-ray crystallographic structures were superimposed for comparison via a least-squares distance minimization of the C_α atoms of the Walker A motif (aa sequence Gx_4GKT) in the P-loop. All rms deviations were less than 0.3 Å in magnitude. Hydrogen-bonding patterns were determined using the hydrogen bond function in the Swiss-PdbViewer, v. 3.01.

RESULTS

Modeling a closed P_i-tube in ncd and docking of nucleotides

Graphical manipulation of molecular structures was done using the MidasPlus molecular visualization system (Ferrin et al., 1988). The protocol to modify the switch 1 region of Dm ncd is summarized in Fig. 1 *B*. Except as noted, only the relevant C_α backbone atoms of the proteins are shown for clarity. The ncd x-ray structure is in gray, except for the magenta switch 1 region, Val 447 and Arg 549. Taking advantage of the structural homology at the nucleotide site, the catalytic domain of myosin, Dd S1·ADP·BeFx (Fisher et al., 1995), was superimposed on monomeric Dm ncd (Sablin et al., 1996) via a least-squares distance minimization of the Walker A motif in the P-loops, aa 434–441 in ncd and 179–186 in Dd S1. The P-loop overlay resulted in the distance between homologous aa 542 in Dm ncd and 228 in Dd S1 and the distance between homologous aa 239 in (S1) and aa 553 (ncd) being less than 0.6 Å (C_α—C_α). In ncd, these residues are located adjacent to the α3-helix and β5-ribbon ends, respectively, of the ncd domain that appears displaced away from the nucleotide in ncd relative to S1. These amino acids were thus taken to define the ends of the switch 1 region. The orange loop shows the location of the switch 1 region of S1 after the overlay of the two proteins. Magenta shows the homologous region of ncd (Fig. 1, *A* and *B*). Starting at the N-terminus end, sequential single-bond, ϕ, ψ bond angle rotations were made manually to the main chain structure of ncd, deforming it to follow as closely as possible the orange, homologous path of S1. Note the close structural homology between the modeled (green) ncd switch 1 and the original, crystallographic template (orange). There is only a 0.5-Å rms deviation (C_α—C_α) between the two switch 1 regions. Following modification of ncd, the C_α—C_β bonds in the ncd side chains pointed in the same general direction as in S1. The ncd side chains (not shown) were subsequently manually rotated by eye to match as best as possible those of S1. There is an ~50% sequence identity between Dd S1 and Dm ncd in the switch 1 region, with no amino acid insertions or deletions. Together with the nucleotide (red), the gray and green portions are seen to constitute an ncd structure with a closed P_i-tube. The green/orange→magenta transition (structurally, a loop→α-helix–loop transition) moves the switch 1 region away from its position covering the phosphates, opening the P_i-tube. It is important to emphasize the significant magnitude of the domain movement we are proposing. The ncd Arg 549 is shown in black with the side chain in both the open and closed P_i-tube, ncd structures. The C_α—C_α distance between Arg 549 in the two configurations is 11.3 Å.

The ncd x-ray structure contained ADP at the nucleotide site. The superposition of ncd and S1 resulted in the P_α—P_α and P_β—P_β distances between the nucleotides in ncd and S1 being less that 0.25 Å. The distance between the respective magnesium atoms was 0.5 Å. Hence, MgATP was docked into both the open and closed P_i-tube ncd structures using the coordinates from MgADP·BeFx (Fisher et al., 1995) in Dd S1 (red, Fig. 1 *B*). The closed ncd structure with bound MgADP was formed using the coordinates for MgADP from the ncd crystal structure (red, Fig. 1 *A*). Except as subsequently noted, no crystallographic waters were retained in any of the structures.

A proposed new structure of a kinesin-family motor is now at hand. We next use MD simulations to analyze both the open and closed P_i-tube structures.

Molecular dynamics of the open, ncd crystal structure

The first MD simulation was of MgADP bound to ncd, using the ncd crystal structure with an open P_i-tube as the initial condition. Fig. 2 shows the rms deviation as a function of time of the C_α atoms in the belly (i.e., the atoms that were allowed to move) from the starting structure. The x-ray

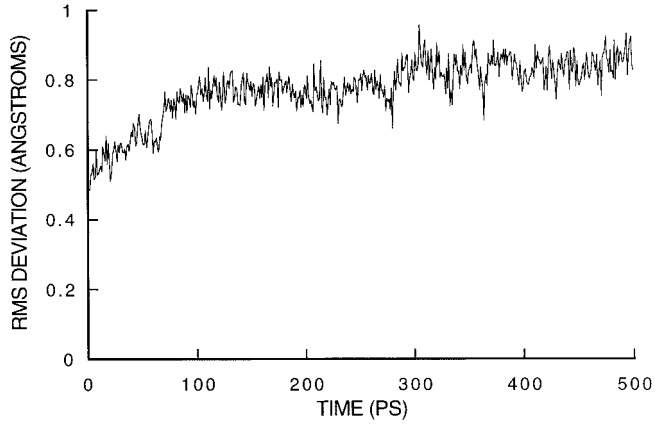

FIGURE 2 Root mean square displacement as a function of time of the MD simulation of ncd with MgADP at the nucleotide site and switch 1 in the open conformation (ncd crystal structure). Approximately 0.5 Å of the rms deviation from the initial structure occurred during the energy minimization steps of the MD simulation. A steady state was reached between 100 ps and 200 ps of MD simulation time.

structure was determined at 100 K. At our higher, 300 K temperature, the MD protein structure remained stable. Approximately half of the total rms deviation of the belly atoms (C_α) occurred during the energy minimization steps. This is the large change of ~0.5 Å at $t = 0$ seen in Fig. 2. There was a subsequent transient change in the position of the belly atoms, with ~90% of the total rms change occurring in the first 100 ps of the simulation. An equilibrium was reached, with only 0.84 ± 0.04 Å rms deviation (mean ± SD) from the initial structure over the final 100 ps of the 500-ps total simulation time (Table 1). This small standard deviation of the aggregate rms deviation allowed us to conclude that the MD had evolved to a stable structure on a 500-ps time scale. We note that similar plots of rms deviations were obtained for subsequent simulations. For brevity, complete data will not be presented, but are summarized in Table 1.

Fig. 3 shows a stereo pair of the evolution of the nucleotide-binding domain in the MD simulation (C_α-backbone). The initial crystal structure (green) and the final time averaged structure from the simulation period 495–500 ps (red) are given. Note that here and elsewhere, unless otherwise indicated, we will refer to the initial structure as the structure for a given simulation before any energy minimization. The final structure will be the structure obtained by averaging the MD snapshots obtained at 1-ps intervals for the simulation period of 495–500 ps. The structures were superimposed at the P-loops. Compared with the initial structure, the ADP and magnesium (not shown) in the final structure shifted by approximately 0.5 Å deeper into the diphosphate-binding domain. More significantly, there was a large displacement and rotation of the ribose and adenine rings relative to the position of the nucleotide in the crystal structure. As seen in Table 1, the small standard deviation of the rms deviation in position of the nucleotide over the final 100 ps again implied that the drifting nucleotide had reached a new, stable position. Switch 2 did not change significantly in the final structure. There was a 1.6-Å rms change in the position of switch 1 in the final structure (C_α—C_α) relative to the initial structure. The largest shift was 2.5 Å at Asn 203. Thus, although switch 1 had clearly moved in the course of the MD simulation, the displacement was not sufficient to form a closed P_i-tube structure.

Additional insights into the relationship between the MD simulation results and the crystal structure can be better understood by comparing the interactions at the nucleotide site in the MD and x-ray structures. Fig. 4 shows the pattern of hydrogen bonding (*dashed lines*) between the protein and MgADP in the final MD structure, as well as some relevant protein-protein coordinations. The magnesium is in magenta. Hydrogen bonds that can be identified in the crystal structure are shown as dashed green lines. Red denotes a hydrogen bond comparable to one seen in the crystal structure, but now water-mediated in the MD simulation. Black lines are hydrogen-bonding patterns in the final MD simulation that cannot be identified in the crystal structure. A hydrophobic stacking interaction between the ring of Tyr 442 in the P-loop and the adenine ring is omitted for clarity. A number of observations are relevant. The primary, direct protein-nucleotide interaction is via the P-loop in both the crystal structure and the MD simulation. With the exception of the ring of Tyr 442 and the water-mediated hydrogen bond from Asp 580 in switch 2, the only crystal structure interactions preserved in the MD simulation are from the P-loop to the diphosphate moiety. Due to the stability of the position of the diphosphates in the MD simulation, these P-loop interactions are preserved, with several new ones established.

The magnitude of the previously noted movement of switch 1 toward the nucleotide is insufficient to allow for direct interactions between MgADP and the main chain or side chains of switch 1. The averaged, final MD simulation shows that instead of direct protein-ligand interaction, a constellation of nine water molecules is established, helping to stabilize the modified position of switch 1 relative to the nucleotide and metal. To be specific, we will define the water constellation to be those waters in the final structure that are part of a hydrogen-bonding chain between the switch 1 region, metal, and ADP involving one or more MD waters. Their coordination is given in Fig. 4. Only two waters in the region of interest can be identified from the ncd crystal structure (green). They are less than 1.1 Å from waters in the overlay of the x-ray crystal and the MD, ncd structures, with identical coordination to Mg^{2+}, P_α, and P_β. We note that for our MD simulations, crystal waters were removed from the structure and a geometric,

TABLE 1 Average rms deviations of the C_α backbone of the belly and the nucleotide (which includes Mg^{2+})

Model	C_α	Nucleotide
ncd + MgADP/switch 1 open	0.77/0.84 (0.09/0.04)	0.84/0.96 (0.11/0.06)
ncd + MgADP/switch 1 closed	0.80/0.87 (0.07/0.04)	0.59/0.71 (0.23/0.09)
ncd + MgATP/switch 1 open	0.78/0.79 (0.04/0.04)	1.03/1.12 (0.24/0.07)
ncd + MgATP/switch 1 closed	1.02/1.16 (0.17/0.05)	0.45/0.44 (0.60/0.05)
ncd/switch 1 open	0.92/0.98 (0.10/0.09)	
ncd/switch 1 closed	0.87/0.95 (0.09/0.03)	

The rms deviations are measured using the initial minimized modeled or, in the ncd + MgADP/switch-1-open case, crystallographic structures as the reference against which snapshots during the MD simulation are compared. Average rms deviations for 500 ps of MD and the last 100 ps are given; σ for each is given in parentheses.

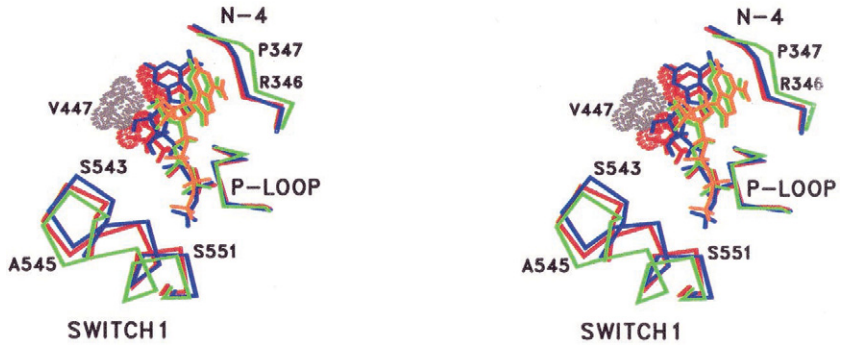

FIGURE 3 Stereo pair of the structure of the nucleotide site (C_α backbone) in the MD simulations with switch 1 in the open conformation. All structures were superimposed on the ncd crystal structure at the P-loops. The crystal structure (initial structure for the MD simulations), including the nucleotide, ADP, is green. ATP in the initial structure is orange. The final MD structure averaged over the simulated time period 495–500 ps (P-loop, switch 1, and loop 1, nucleotide) for ADP (ATP) is red (blue). The adenine and ribose in the final structures are rotated and displaced relative to their initial locations. In the final ADP structure, the van der Waals surface for the methyl groups of Val 447 (gray) and the abutting van der Waals surfaces of the ribose and adenine moieties of ADP (red) are also shown. The displacement of the N-4 domain during the MD simulations is shown at the upper right.

space-filling algorithm was then used to re-hydrate the protein. The above two waters were then required to "find their way home on their own," providing additional confidence in our simulations.

The question remains as to why two members of the water constellation are seen in both the MD simulation and x-ray structure, whereas the remaining constellation waters in the MD simulations are not seen in the crystal structure. A potential answer can be found by examining the motion of these waters as a function of time. Over the 5-ps time period for which positions were averaged for the final structure, the rms deviations from their average position for all of the nine constellation waters was less than 0.53 Å. The data of Fig. 2 (rms deviation of the entire belly) implied that the protein had reached an equilibrium configuration by 300 ps of the MD simulation. Looking at the last 200 ps, the rms deviations of the two waters mimicking the crystal structure increased to only 0.6 Å. The remainder of the water molecules, however, had rms deviation values ranging between 1.7 and 6.5 Å (4.0 ± 0.8 Å, mean ± SEM) over the final 200 ps. For relative comparison, the metal and P_β had rms deviations of only 0.26 and 0.28 Å, respectively, over the last 200 ps of MD. Thus, the simulation data imply that although the position of the two waters interacting with the metal and identified in the crystal structure are fairly immobilized, the remainder of the water constellation has considerable long-term mobility, with water molecules moving in and out. These would not be picked up by x-ray crystallography. The long-term mobility of water constellations at the nucleotide site also has important implications for nucleotide hydrolysis and will be addressed in the Discussion.

Simulation of MgATP docked to the crystal structure

ATP is ~3 Å longer than ADP. Can additional protein-nucleotide interactions be generated by the γ-P_i of ATP and result in a closing of the P_i-tube? The MD simulations with MgATP at the nucleotide site of the crystal structure indicated that the switch 1 region remained in the open conformation. The final averaged ATP structure is shown in Fig. 3 (blue). Over the final 100 ps, the MD structure had a rms deviation from the initial configuration of 0.79 ± 0.04 Å (mean ± SD; Table 1). Approximately 50 ps of simulation time was required to reach this equilibrium configuration (data similar to Fig. 2 and not shown) indicating that the MD structure is stable on our 500-ps time scale. For ATP in the final structure (blue), there was again a shift of the triphosphates deeper into the open P_i-tube. The magnitude of the displacement was slightly larger than observed with MgADP, with a corresponding increase in the rms deviation from the initial position of ATP (Table 1) when compared with the ADP simulation. Again, there was a significant displacement and rotation of the base and sugar. The small standard deviation of the rms position deviation over the last 100 ps (0.07 Å, Table 1) implied that the displaced nucleotide was at a stable location.

An analysis of the final structure as in Fig. 3 (data not shown) indicates that the primary direct hydrogen bonding to the metal-nucleotide complex is again from the P-loop, with one water-mediated and nine direct hydrogen bonds. The open switch 1 region has a rms deviation of 1.9 Å (C_α—C_α) from the crystal structure, again displacing toward the nucleotide. The maximum displacement is 2.85 Å at Gly 546 (C_α—C_α). The γ-P_i of ATP results in the nucleotide being closer to switch 1 than with ADP. It is still not close enough, however, for direct hydrogen bonding from the protein to the nucleotide. At closest approach, a rotation of the position of the side chain of Ser 551 toward ATP in the final MD simulation would still leave a 3.7-Å distance from the hydroxyl hydrogen to the nearest γ-P_i oxygen. Instead, coordination between the open switch 1 region and the nucleotide is again established via a constellation of eight water molecules. The rms deviations of these waters from their average position over the last 5 ps of

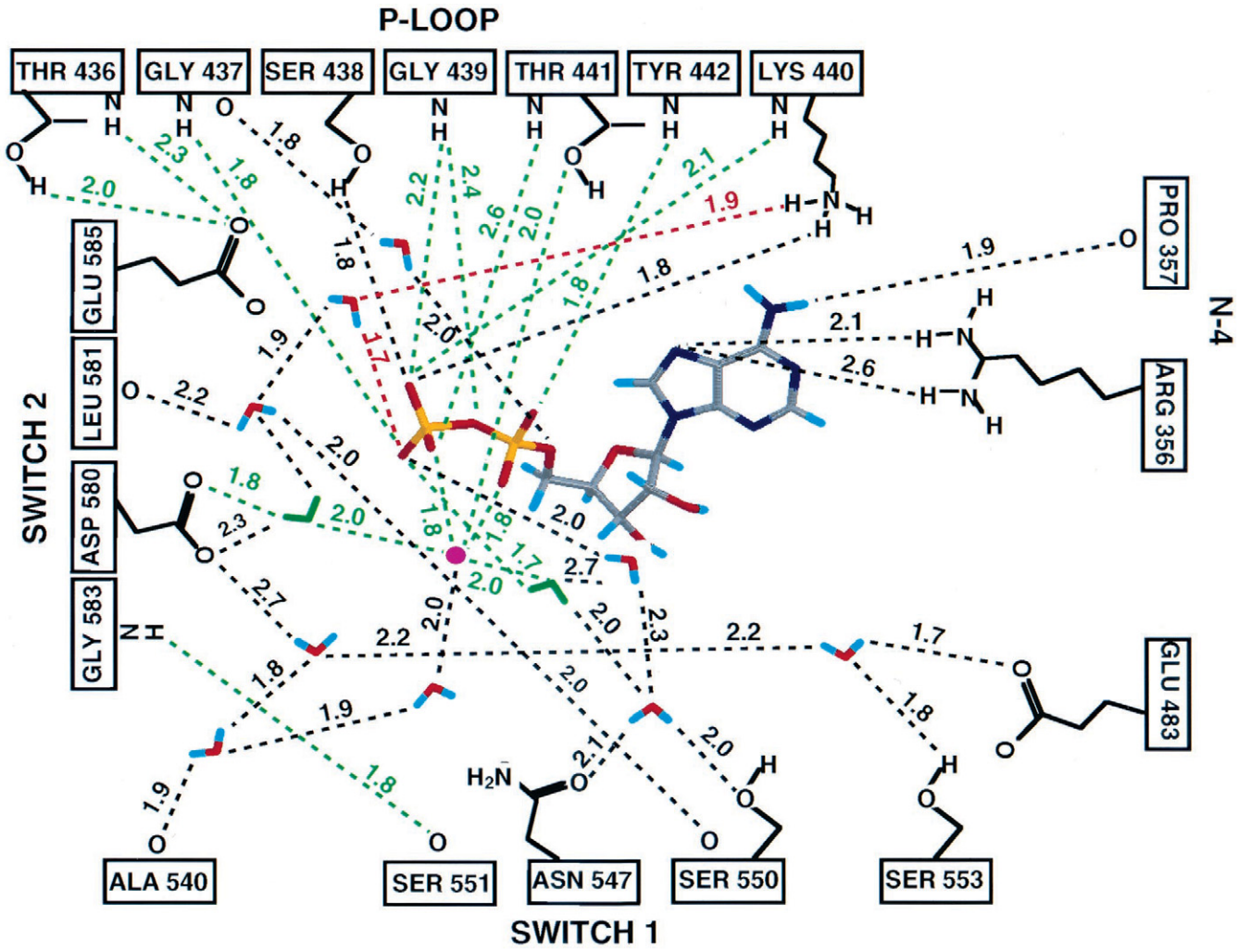

FIGURE 4 The schematic of the coordination of the nucleotide to ncd and intra-protein coordination in the MD structure averaged over the simulated time period 495–500 ps. The color scheme for the nucleotide and waters is carbon, gray; nitrogen, dark blue; oxygen, red; phosphorus, yellow; hydrogen, cyan. The magenta circle is magnesium. Two waters identified in the crystal structure are green. The dashed lines give hydrogen bonding/ionic interactions with distances in angstroms. A 2.7-Å cutoff was used for nonbonded interactions. Green lines indicate interactions identified in the monomeric Dm ncd crystal structure. Red lines indicate a protein-nucleotide interaction in the x-ray structure that has been modified to include a water intermediate in the MD simulation. Black lines indicate interactions that are not identified in the crystal structure. The hydrophobic interaction of the ring of Tyr 442 with the adenine ring is not shown. For purposes of clarity, the drawing is not to scale and some amino acids are displayed out of sequential order.

simulation vary from 0.18 to 0.94 Å (0.52 ± 0.09 Å, mean ± SEM). Over the final 200 ps of the simulation, all rms deviation values are greater that 1.1 Å (2.9 ± 0.9 Å, mean ± SEM). The corresponding reference values for Mg^{2+} and P_γ are 0.24 and 0.25 Å, respectively. We again conclude that with MgATP at the nucleotide site and switch 1 in the open configuration, a water constellation is formed that displays short- but not long-term stability.

Molecular dynamics simulations of ncd with a closed P_i-tube

We next examine the properties of our hypothesized ncd structures with the switch 1 region modified to form a closed P_i-tube. This requires a large displacement of the switch 1 region. Two questions become relevant. Is the closed P_i-tube structure even stable under MD? Does the modeled, closed Pi-tube reopen during MD? The closed P_i-tube structure was constructed based upon a Dd S1·nucleotide triphosphate analog structure (Fisher et al., 1995). We thus discuss this structure first.

Simulation of MgATP in a closed P_i-tube, ncd structure

In the MD simulations with MgATP, the position of the switch 1 remains in the closed conformation (see Fig. 5), with the final structure (red) having only a 2.4-Å rms

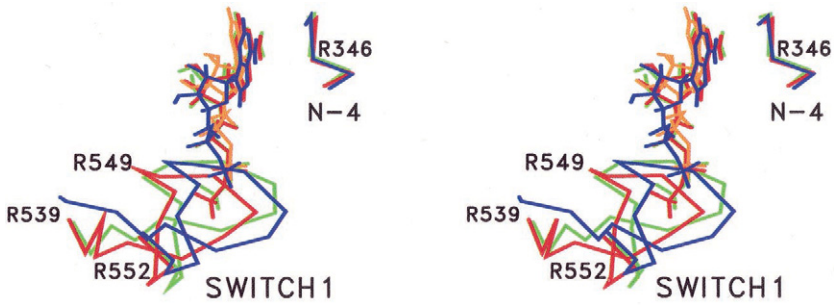

FIGURE 5 Stereo pair of the structure at the nucleotide site in the MD simulations with switch 1 in the closed conformation with ATP and ADP at the nucleotide site (C_α protein backbone). All structures were superimposed on the modeled ncd structure with switch 1 closed using a least-squares distance minimization on the C_α atoms of the P-loops. The initial location of switch 1 is in green (both simulations), ADP is in orange, and ATP is in green. In the final averaged structure (simulation period 495–500 ps) with ATP (ADP) at the nucleotide site, switch 1 and the nucleotide are shown in red (blue). The N-4 domain is at the upper right. Residue identifications are with respect to the final, red, structure.

deviation from its position in the initial (green) structure (C_α—C_α) and uniformly displacing away from the nucleotide γ-P_i (maximum displacement of 3.9 Å at Ala 545). The MD simulations imply that the closed P_i-tube structure is stable on a 500-ps time scale (rms deviations, Table 1). The displacement of the adenine and ribose rings observed in the closed P_i-tube simulations are dramatically reduced when compared with the open configuration (Fig. 3). The closed P_i-tube surrounding the triphosphates also stabilizes the nucleotide, reducing its rms deviation by a factor of two relative to that in the open P_i-tube structure.

The coordinations of the protein to the nucleotide in the final MD structure, Fig. 6, help to explain the differences we see relative to the open switch 1 simulation. Amino acids that are conserved between Dd S1 and Dm ncd are labeled in green. Water molecules that are in the template, S1·ADP·BeFx structure and in our final MD ncd structure (distance offset less than 1.2 Å in the superimposed structures and with identical coordinations) are colored green. Hydrogen bonds that can be identified between conserved amino acids, equivalent waters, the metal, and the nucleotide in both the S1 (see Fig. 6) (Fisher et al., 1995) and the final MD ncd structure are colored green. Hydrogen bonds to the nucleotide in the ncd structure that have comparable interactions in S1 are colored red. Thus, red represents either a change in water mediation of the hydrogen bond or a substitution of a different amino acid in the ncd sequence. Hydrogen bonds that have no equivalent in S1 are colored black. We again note that S1 crystal waters were removed for the simulation and the protein resolvated solely on the basis of a geometric algorithm. Reestablishment of their location in the MD simulation was solely the result of intermolecular forces. The important point in Fig. 6 is that the preponderance of protein-metal-ligand interactions are either green or red, indicating that the MD coordination found in a kinesin-family motor is remarkably similar to that identified in an x-ray crystal structure. The extensive interaction with the P-loop observed in the open P_i-tube simulation remains. The water constellation between the nucleotide and switch 1 is gone, however, with the closed structure now showing direct interaction between the Mg^{2+}, nucleotide, and switch 1.

MgADP in the closed P_i-tube structure

The initial and final positions of the modeled ADP are shown in Fig. 5, orange and blue, respectively. There is again a dramatically reduced motion of the adenine and ribose when compared with the open conformer. The relationship of the initial (green) and final (blue) locations of the switch 1 region is comparable to that observed with MgATP at the nucleotide site. The C_α rms displacement of the switch 1 region is slightly less than with ATP, 1.6 Å (maximum displacement of 2.3 Å at Gly 202). Amino acids 542–543 and 549–553 are displaced toward the nucleotide relative to the initial structure, aa 544–548 away from the nucleotide. The rms deviations of the belly C_α atoms and the nucleotide (Table 1) again indicate that the final MD structure with closed P_i-tube is stable. The rms deviation of the nucleotide over the last 100 ps of the simulation is again reduced from that observed in the open switch 1 conformation as shown in Table 1.

The terminal P_β of ADP is located 2.4 Å less deep in the P_i-tube that of the ATP terminal P_γ. The initial location of the switch 1 region was based upon a triphosphate analog x-ray structure. The displacement of aa 549–553 (containing the conserved SSR motif in switch 1) toward the nucleotide thus appears required to maximize interaction with the nucleotide. This movement results in a somewhat more tightly closed P_i-tube in the simulated ADP structure than with ATP.

An analysis of the protein-metal-ligand coordination for the final closed- P_i-tube structure with bound MgADP as in Figs. 4 and 6 (data not shown) also indicates considerable similarity with that identified in the Dd S1·ADP structure (Gulick et al., 1997). In both MD and the x-ray structures, the metal coordinates only to the P_β of the nucleotide. All five of the hydrogen bonds from the switch 1 region to the metal-nucleotide complex in the MD simulation are also found in the S1·ADP crystal structure, although two of these are water-mediated in the S1·ADP structure. There are eight direct hydrogen bonds from the P-loop to the nucleotide triphosphates in the final MD structure. Six of these are identical to hydrogen bonds in the crystal structure. Thus,

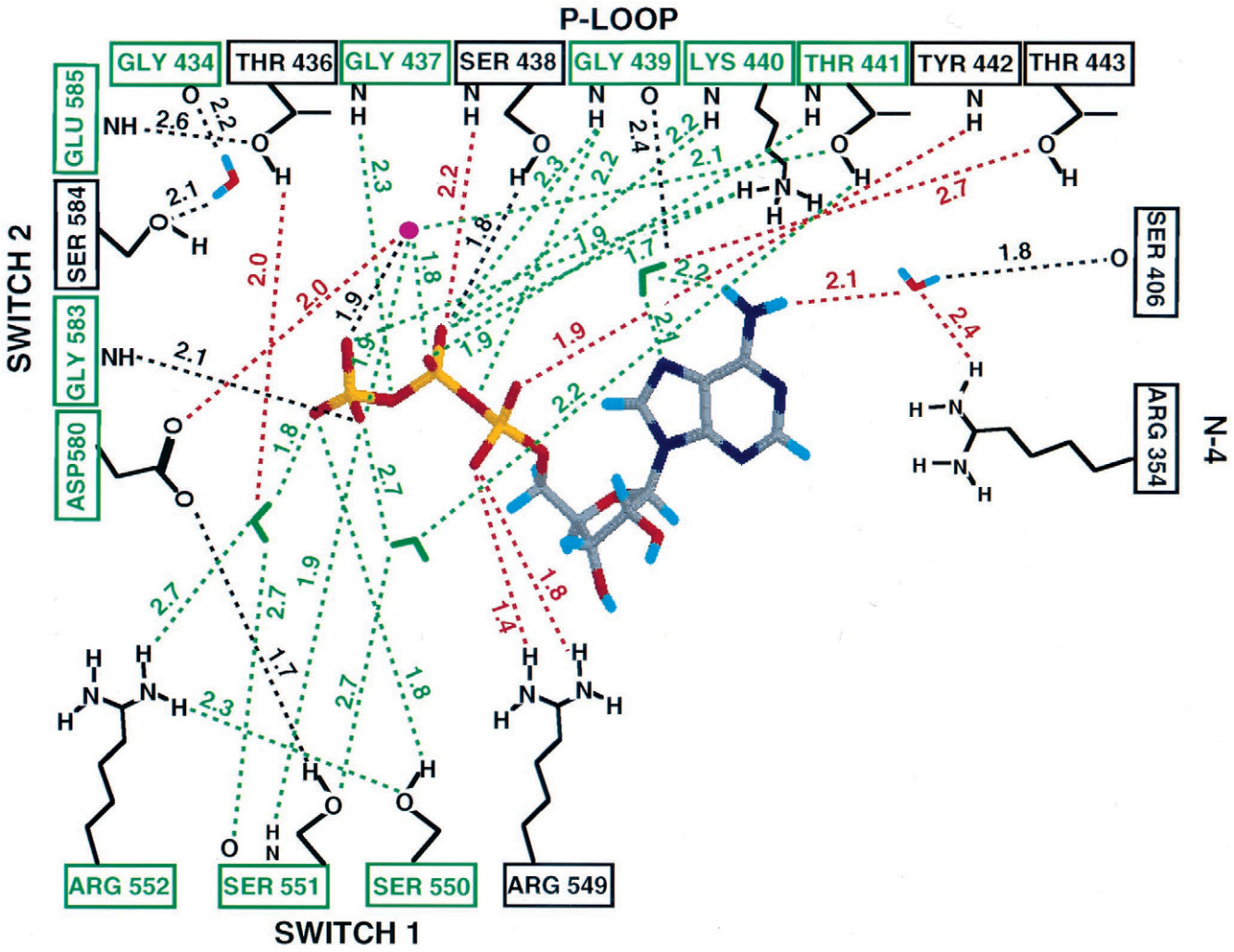

FIGURE 6 The schematic of the coordination of MgATP to ncd and intra-protein coordination in the MD structure for the ATP-closed simulation averaged over the time period 495–500 ps (final structure). The color scheme for the nucleotide and waters is as in Fig. 4. The magenta circle is magnesium. The coordination of protein and nucleotide is compared with that found in the Dd S1·ADP·BeFx structure of Fisher at al. (1995). This is the structure that provided the template for the closing of switch 1 in ncd. Amino acid residues that are conserved between Dd S1 and Dm ncd are labeled with green boxes. Green dashed lines indicate interactions identified in both the Dd crystal structure and the ATP-closed MD simulation. Red lines indicate an interaction in S1 that involves a different amino acid residue in ncd or has been modified to include a water intermediate. Black lines indicate interactions in ncd that are not identified in the S1 crystal structure. A 2.7-Å cutoff was used. The hydrophobic interaction of the ring of Tyr 442 with the adenine ring is not shown. For purposes of clarity, the drawing is not to scale and some amino acids are displayed out of sequential order.

we conclude that the MD simulation predicts coordination similar to that seen the in the Dd S1·ADP crystal structure.

Effect of the opening and closing of the switch 1 region on the positioning of the adenine and ribose rings

The interaction between ncd and the adenosine portion of ADP is rather pathetic in the Dm ncd crystal structure. No interaction with the ribose can be identified. The adenine ring is positioned in a hydrophobic slot consisting of the ring of Tyr 442 on one side and the side chain of Arg 356 on the other. Arg 356 is the amino terminus of the conserved, RxRP motif (aa 356–359) found at the junction of the β-ribbon, β1, and loop, L1. This motif is frequently referred to as N-4 (Vale, 1996; Sack et al., 1999), and we adopt this notation here. In G-proteins, the structurally homologous NKxD motif hydrogen bonds to the 6-position carbonyl and 2-position amino group of the guanine ring, enhancing substrate specificity and potentially suggesting a more specific role for N-4 in ncd. We examine this possibility here.

In the Dm ncd crystal structure, the position of the side chain of Arg 356, one side of the hydrophobic adenine slot, is stabilized by a hydrogen bond from the N_ξ hydrogen to the backbone oxygen of Pro 357, by a hydrogen bond from

a terminal amino side-chain hydrogen to the backbone oxygen of Gly 437 in the P-loop, and by an interaction from a hydrogen on the other side-chain terminal amino group to a side-chain oxygen of Glu 362. There is a major difference between the structures with the switch 1 region in the open or closed conformations, as seen by comparing Figs. 3 and 5. In the open structure, there is a movement of the adenine ring out of the hydrophobic slot and a large rotation of the plane of the ring for the MD simulations with both ATP (4.5 Å, C_6—C_6; 50° rotation) and ADP (3 Å; 70°). The ring of Tyr 442 translates and rotates to preserve hydrophobic stacking in the final structures. The other hydrophobic interaction with the side chain of Arg 356 is lost. Instead, in the ADP structure, a hydrogen-bonding pattern from the adenine is established to an amino group of Arg 356 and to a backbone oxygen of Pro 357 (see Fig. 4). More importantly, this change in coordination is accompanied by a movement of N-4 and adjacent residues (rms deviation from original structure of 1.5 Å for aa 354–362; maximum movement of 1.8 Å for Arg 359, all based upon C_α), partly closing the nucleotide pocket (Fig. 3). The MD simulation with ATP at the active site and switch 1 in the open configuration shows similar behavior. In the altered position, the adenine also hydrogen bonds with Arg 356 and Pro 357 (not shown), similar to ADP, with comparable displacement of the N-4 domain (Fig. 3). The C_α rms deviation of N-4 from the crystal structure is 1.5 Å, with maximum displacement (C_α—C_α) of 2.0 Å at Pro 357. These observations are the first evidence based upon an argument other than sequence and structural homology with G-proteins that interaction of the universally conserved N-4 motif in kinesin-family motors with the nucleotide can induce a conformational change in the protein.

In their final positions, the adenine and ribose positions are stabilized by two factors. One is hydrogen bonding from Arg 356 and Pro 357 (Fig. 4). More importantly, further sideways displacement of the adenine and ribose out of the nucleotide pocket is now prevented by new van der Waals contact with the protein (Fig. 3). In the ADP structure, the 2′,3′-ribose hydroxyl hydrogens, along with the C_2 hydrogen and N_3 of the adenine ring, have van der Waals contact with the methyl groups of Val 447 and a C_β hydrogen of Tyr 442 (latter not shown in Fig. 3). The phosphate end of the nucleotide is tethered due to the extensive interaction with the P-loop. Fixed by this tethering, the additional van der Waals contact prevents the nucleotide from further sideways sliding out of the nucleotide pocket. With ATP at the active site, similar interference by Val 447 occurs with the adenine N_3 and with the C_2 hydrogen of the adenine ring; the C_β hydrogen of Tyr 442 additionally blocks at the O_3' position on the ribose ring (not shown). Val 447 is located on the side of the extremely peculiar β-hairpin protruding from the α2-helix at the C-terminus side of the P-loop (see Fig. 1A). This β-hairpin is structurally conserved in all kinesin-family x-ray structures to date, but is lacking in the homologous α-helices in all myosin and G-protein structures. Its function is unknown. The present simulations provide the first evidence linking it to nucleotide binding.

To the contrary, the adenine and ribose moieties stay more or less fixed in the closed P_i-tube structures. The reason is switch 1. To close the P_i-tube, the switch 1 region moves in toward the nucleotide by ~10 Å. The side chain of Arg 549 now points directly at the nucleotide and hydrogen bonds to a P_α oxygen with ATP at the nucleotide site (Fig. 6) or to the adjacent ribose O_3' with ADP (data not shown). These interactions, along with van der Waals interference from the adjacent Asn 548, prevent displacement of the ribose ring. Accompanied by hydrophobic forces at the adenine ring slot, these are now sufficient to stabilize the position of the nucleotide. Viewed another way, in the closed conformation, switch 1 physically blocks the sideways displacement of the nucleotide. In the switch-1-open conformation, the minimal cohesiveness of the interposed water constellation is insufficient to prevent nucleotide drift. We note that the binding of nucleotide to S1 likewise shows few protein-mediated interactions with the adenosine moiety in the x-ray structures. Nonetheless, our previous MD simulations at 300 K with the closed P_i-tube, Dd S1·ATP and S1·ADP structures (Minehardt et al., 2000) also failed to show any nucleotide drift, suggesting a more general result for closed switch 1 structures.

Can the differences in the location of the nucleotides in the ncd x-ray structure and in the MD switch-1-open simulations be reconciled? Additional simulations including explicit crystal waters at the nucleotide site, one involved in a hydrogen bond between the adenine and the protein, showed identical nucleotide drifts. This argues that it is not our improper handling of water that is causing the difference. One other difference is that the x-ray data were collected at 100 K, as opposed to 300 K for the MD results. Thus, we performed an additional MD simulation identical to the one above with an open P_i-tube and ADP modeled at the nucleotide site, but at 100 K. The nucleotide position after 500 ps of simulation time was then compared with its starting position and with that obtained in the ADP-closed simulation at 300 K. The adenine ring in ADP rotated only 10° relative to its starting position, with the adenine heavy atoms displacing a mean of 1.5 Å. As discussed previously, this was roughly the displacement observed in the adenine ring in the ADP-closed MD simulation, 300 K. Indeed, the rms deviation in the final structures between the heavy atoms in the adenine ring for the simulation at 100 K with the switch 1 region open and the simulation at 300 K with the P_i-tube closed was only 0.54 Å. Furthermore, the lack of change in position at the lower temperature with switch 1 open cannot be attributed solely to the lower temperature freezing out all molecular motion. The adenine ring did displace, by an amount comparable to that observed at the higher temperature, 300 K, with switch 1 closed, but only for the initial 100 ps of simulation time. After that, the new

and final equilibrium was reached. This is roughly the time for equilibration of the rms deviation in position for the closed configuration at the higher temperature, 300 K. The new equilibrium position was thus stable on our 500-ps time scale.

We conclude that the kinesin-family motor crystal structures may be quite unrepresentative of the position of the nucleotide in the active site at physiological temperatures. Indeed, if the ncd motor cycle does require the protein to spend a significant fraction of time in a configuration with the switch 1 region pulled back from the nucleotide as in the x-ray structures, maintenance of long-term nucleotide binding would appear problematical. The β-hairpin in the α2-helix may have evolved simply to serve as a bumper stop, enhancing stability of the nucleotide-bound state with the switch 1 region in the open conformation. At a minimum, our proposed movement of the switch 1 region to close the P_i-tube would appear to dramatically enhance the positional stability of the bound nucleotide at more physiological temperatures.

Influence of switch 1 on movements of the switch 2 region

We examine here the relationship between the position of the switch 1 region, the nucleotide phosphates, and movements of switch 2. Although large-scale movements of switch 2 have been seen in S1, and postulated to be involved in the power stroke, no comparable movements have been seen in the kinesin-family motors. Switch 2 is within the belly of the MD simulations.

The important observation from Fig. 7 is that there is a significant displacement of switch 2 toward P_γ, but only in the ATP-closed simulation. Fig. 7 shows the relationship between switch 2 (C_α atoms), the nucleotide, and the conformation of the switch 1 region in the ADP- and ATP-open and -closed MD simulations. All structures are shown superimposed on the Dm ncd crystal structure. The ncd switch 2 locations from the four ncd simulations fall into two distinct classes (Fig. 7, *B* and *C*). The initial location of switch 2 in the ncd crystal structure is in class *B*, green. Three final MD simulations, ADP-open (gray), ADP-closed (red), and ATP-open (magenta) also are in class *B*. The other ncd final structure, ATP-closed, is in an entirely different position, colored red in class *C*. The C_α rms deviation from the initial crystal structure position for ATP-closed is 2.8 Å, with a maximum displacement of 5.2 Å at Glu 584. This compares with a $<$0.6-Å rms deviation from the crystal structure position of switch 2 for the other three simulations in class *B*. The other switch 2 domains in Fig. 7 are from other structures and will be considered in the Discussion.

Why does the switch 2 translation occur only for ncd·ATP with the P_i-tube closed? How does the position of switch 1 influence the position of switch 2? As seen in Fig. 4 (ADP-open) and Fig. 6 (ATP-closed), there is a significantly different coordination of switch 2 to switch 1 and the nucleotide in the ATP-closed state. The crystal structure of ncd shows a hydrogen bond between the backbone amino group of the conserved Gly 583 in switch 2 and the backbone oxygen of the conserved Ser 551 in switch 1 (magenta G583, class *B*, Fig. 7). By our simulation protocols, this hydrogen bond is preserved in the initial structures for all of the switch-1-open simulations. In the process of modifying and closing switch 1, however, the backbone oxygen of Ser 551 in the switch 1 region was displaced by 2.5 Å, breaking this hydrogen bond. In the ATP-closed simulation, this allows the backbone amide of Gly 583 to assume a new

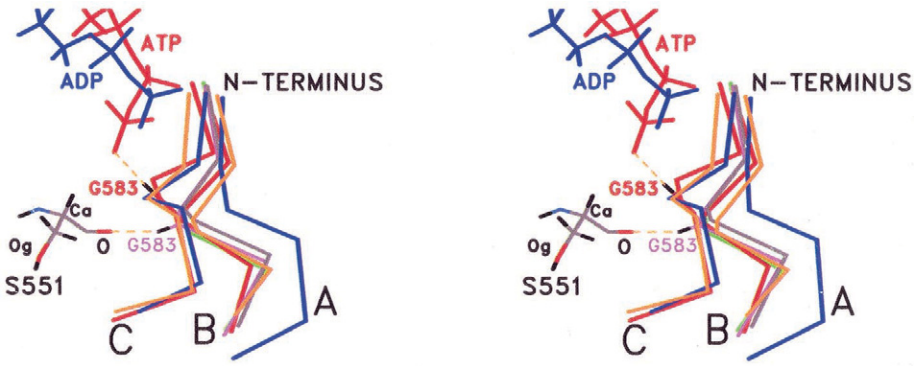

FIGURE 7 Stereo pair of the C_α backbone of switch 2 in three distinct conformations. MD simulations termed final are the average of the position over the period 495–500 ps. (*A*) Switch 2 from Dd S1·ADP·BeFx structure. (*B*) Switch 2 from human kinesin (orange); ADP-open final (gray); ADP-closed final (red); ATP-open final (magenta). (*C*) ATP-closed final (red); Dd S1·ADP·AlF^{4-} (blue); smooth muscle S1·ADP·BeFx (orange). The phosphate portions of ATP (ATP-closed, final) and ADP (ADP-closed, final) are at the top. The hydrogen bonding of the backbone amino group hydrogen (black) of Gly 583 for the ATP-open structure is also shown. In all final MD structures for Dm ncd, except for the ncd ATP-closed final structure, there is a hydrogen bond between the backbone amino group hydrogen of Gly 583 and the backbone oxygen (red) of Ser 551. In the ATP-closed final structure, the amino group of Gly 583 translates and rotates to form a new hydrogen bond with the γ-P_i of ATP. For Ser 551, carbons are colored gray, oxygens red, hydrogens black, and nitrogen blue.

coordination, displacing by 1.8 Å and rotating by 75° to form a new hydrogen bond with a γ-P_i oxygen of ATP (red G583, class *C*, Fig. 7). This change in coordination from Ser 551 to Gly 583 is demonstrated in Fig. 7. Additional stabilization of the new switch 2 location in the ATP-closed simulation is provided by hydrogen bonding between Asp 580 and the side-chain hydroxyl of the newly located Ser 551. Additionally, there is a replacement of a side-chain hydrogen bond between Glu 585 in switch 2 and Thr 436 in the P-loop by a shorter, backbone hydrogen bond (all shown in Fig. 6). In the ADP-closed simulation, Gly 583 is also not initially coordinated to Ser 551. However, due to the reduced length of the diphosphate moiety, the P_β is too far from Gly 583 for the change in coordination to occur as did with ATP, and movement of switch 1 during the MD simulation actually reestablishes the backbone coordination of Gly 583 and Ser 551 (the hydrogen bond to Ser 551 shown in Fig. 7). In the ATP-open simulation, the location of Gly 583 is stabilized by the preexisting hydrogen bond to Ser 551. The only coordination between Asp 580 and Ser 551 evident after 500 ps of MD is via a two-water chain in the water constellation between switch 1 and the nucleotide. Thus, switch 2 does not move with switch 1 open and ATP or ADP at the active site.

Analyses of the energetics of the structures

The MD simulations indicate that the four structures we have discussed are all thermodynamically stable on the 500-ps time scale of our simulations. This would imply that each MD trajectory arrives at a topology that represents a distinct local minimum on a much larger potential energy surface. Here we examine the energetics of the states to better understand the relationships between the open- and closed-P_i-tube conformations.

As described in Methods, we have calculated the energies of the ATP- and ADP-open and -closed conformations. The values for the individual components of the conformational energy for protein, ligand, and complex are in Tables 2 and 3, with the sum, $E_{\text{total, PB}}$, as the last line of each column. For the cases with MgADP as the nucleotide, the total energy of the complex with switch 1 open is clearly energetically preferable to the closed conformation, -14391 ± 25 vs. -14287 ± 22 kcal/mol. The lower energy provides a potential explanation for the open phosphate-binding domain observed in the ncd crystal structure. With MgATP at the nucleotide site, the closed and open conformers are of roughly equal energy, -14782 ± 21 vs. -14766 ± 23 kcal/mol. The greater charge density of MgATP, along with the increased communication between the closed switch 1, is why the situation changes when MgADP is the ligand.

Energies for the binding of MgATP and MgADP to ncd calculated from Eq. 2 are presented by component in Table 4. The table shows that ΔE_{bind} is lower for the ADP and ATP structures with closed P_i-tubes than for the corresponding open structures. This is reassuring. We have shown that increased communication between the nucleotide and charged or polar moieties present in switch 1 is an obvious result of the closing of switch 1. The electrostatic terms dominate the binding energy calculations, compensating for unfavorable solvation free energies. It is also worthy of note that in cases where switch 1 is open, the total solvation and electrostatic energies are positive. When the switch is closed, the electrostatic term is more favorable than the PB term, and thus the total PB and electrostatic energies are negative quantities.

The binding free energy of nucleotide to ncd has not been experimentally measured. However, by comparison with myosin, it can be expected to be in the range of -10 to -15 kcal/mol under physiological conditions (reviewed in Taylor, 1979). Given the approximate nature of our methods, and considering the finite number of snapshots that can be analyzed in a reasonable time, Table 4 shows good agreement between those experimentally determined values and our calculated values for the MD simulations. The corresponding values for S1 and the modeled open structures differ by only about a factor of 2. The model values for the closed conformers are somewhat higher, -51 and -73

TABLE 2 Energies (SD) for the two MgADP ncd models

	MgADP/switch 1 open			MgADP/switch 1 closed		
	Receptor	Ligand	Complex	Receptor	Ligand	Complex
$E_{\text{electrostatic}}$	−11761 (26)	−843 (9)	−12834 (27)	−11748 (19)	−724 (11)	−12959 (22)
E_{vdW}	−1371 (12)	26 (4)	−1379 (10)	−1302 (14)	13 (3)	−1321 (15)
E_{internal}	3388 (21)	56 (5)	3444 (21)	3496 (24)	52 (5)	3547 (26)
E_{MM}	−9744 (30)	−761 (11)	−10769 (36)	−9556 (31)	−659 (7)	−10733 (25)
E_{nonpolar}	84 (0.2)	4 (0.02)	84 (0.3)	85 (0.2)	4 (0.02)	83 (0.3)
E_{PB}	−3629 (18)	−321 (8)	−3706 (17)	−3694 (15)	−416 (8)	−3637 (19)
$E_{\text{solvation}}$	−3545 (18)	−317 (8)	−3622 (17)	−3610 (15)	−412 (8)	−3554 (19)
$E_{\text{PB+electrostatic}}$	−15391 (22)	−1165 (5)	−16540 (22)	−15443 (18)	−1140 (5)	−16597 (23)
$E_{\text{total,PB}}$	−13289 (24)	−1079 (6)	−14391 (25)	−13165 (24)	−1071 (2)	−14287 (22)

Quantities are in kcal/mol and SDs are in parentheses. Ten snapshots from the 300–500-ps segment of the MD runs were used for the data analyses presented in this table. See the text for definitions of the energetic terms.

TABLE 3 Energies (SD) for the two MgATP ncd models

	MgADP/switch 1 open			MgADP/switch 1 closed		
	Receptor	Ligand	Complex	Receptor	Ligand	Complex
$E_{electrostatic}$	−11649 (31)	−1253 (11)	−13233 (24)	−11632 (35)	−1228 (11)	−13365 (31)
E_{vdW}	−1346 (11)	38 (5)	−1342 (11)	−1334 (21)	29 (5)	−1346 (18)
$E_{internal}$	3435 (21)	73 (4)	3508 (22)	3467 (20)	69 (5)	3535 (22)
E_{MM}	−9560 (42)	−1143 (6)	−11066 (40)	−9500 (37)	−1131 (6)	−11176 (27)
$E_{nonpolar}$	85 (0.2)	4 (0.02)	84 (0.3)	84 (0.3)	4 (0.03)	83 (0.3)
E_{PB}	−3724 (28)	−395 (7)	−3785 (24)	−3759 (28)	−408 (7)	−3688 (22)
$E_{solvation}$	−3639 (28)	−390 (7)	−3700 (24)	−3674 (28)	−403 (7)	−3605 (23)
$E_{PB+electrostatic}$	−15374 (17)	−1648 (7)	−17017 (12)	−15391 (16)	−1636 (7)	−17053 (17)
$E_{total,PB}$	−13199 (23)	−1533 (2)	−14766 (23)	−13174 (22)	−1534 (4)	−14782 (21)

Quantities are in kcal/mol and SDs are in parentheses. Ten snapshots from the 300–500-ps segment of the MD runs were used for the data analyses presented in this table. See the text for definitions of the energetic terms.

kcal/mol for ATP and ADP, respectively. When switch 1 is closed, more direct contacts are present between the protein and the ligand. Looking at the change in binding free energies for open and closed states we see as expected that the binding to the nucleotide is more favorable when switch 1 is closed in general and when MgATP is the ligand in particular.

Two additional factors must be considered in assessing the binding energies. For ligands the size of ADP and ATP, $-T\Delta S$ would be expected to be in the range of +20 to +30 kcal/mol (Massova and Kollman, 1999; Chong et al., 1999). Thus, adding terms of this magnitude to the calculated ΔG would bring them closer in magnitude to experiment. Of course, the absolute binding free energies are also sensitive to the value chosen for the radius of the magnesium. Nonetheless, it is clear that our values for binding free energies are in the right order of magnitude compared with experiment.

MD of the transition between the closed and open switch 1 structures

Simulated annealing was used to test further the hypothesis that the open and closed switch 1 conformations represented local free energy minima. The initial condition for this simulation was identical to the initial condition for the ATP- or ADP-closed structures, except that the nucleotide was omitted. Following energy minimization and addition of waters, a repetitive sequence of 100 ps of MD followed by a 100 K increase in simulation temperature was performed until the temperature had been increased from 300 K to 800 K. After 100 ps of MD at 800 K, the temperature was decreased to 300 K and a final 500 ps of MD was done. The nucleotide was omitted in this simulation because it was observed to drift out of the nucleotide site at high temperatures. Fig. 8 shows the evolution from the closed to the open configuration. The initial closed switch 1 (green) has opened at 800 K (blue) and remains open when cooled back to 300 K (red). An additional control showed that the closed, apo structure remained closed and stable for 500 ps of MD simulation at 300 K. Thus, the important observation is that as expected from our hypothesis of multiple stable states, we have simulated a closed, stable configuration of the switch 1 region transforming into a stable, open configuration. The maximum switch 1 region displacement from the initial, closed conformation is 14.4 Å at Ala 545. The final open-configuration switch 1 region is similar but not identical to that of the ncd crystal structure (magenta), with a 4.8-Å C_α rms deviation. This is not an unexpected outcome because the crystal structures of monomeric Kar3, kinesin, and ncd also show comparable differences in the location of their switch 1 regions. This further supports the

TABLE 4 Binding energies (SD) for four ncd models considered in this study

	ADP (O)	ADP (C)	ATP (O)	ATP (C)
$E_{electrostatic}$	−229 (14)	−486 (18)	−330 (14)	−505 (18)
E_{vdW}	−34 (6)	−32 (5)	−33 (4)	−41 (4)
E_{MM}	−263 (11)	−518 (14)	−363 (14)	−546 (19)
$E_{nonpolar}$	−5 (0.1)	−6 (0.3)	−5 (0.1)	−6 (0.1)
E_{PB}	245 (11)	473 (18)	334 (13)	478 (13)
$E_{solvation}$	240 (11)	468 (18)	329 (13)	472 (13)
$E_{PB+electrostatic}$	16 (7)	−13 (8)	4 (6)	−27 (12)
$E_{total,PB}$	−23 (4)	−51 (7)	−35 (5)	−73 (13)

In the column headers, O refers to the switch 1 open conformer and C to the switch 1 closed conformer. Ten snapshots from the 300–500-ps range were used in the calculations. See the text for definitions of the energetic terms.

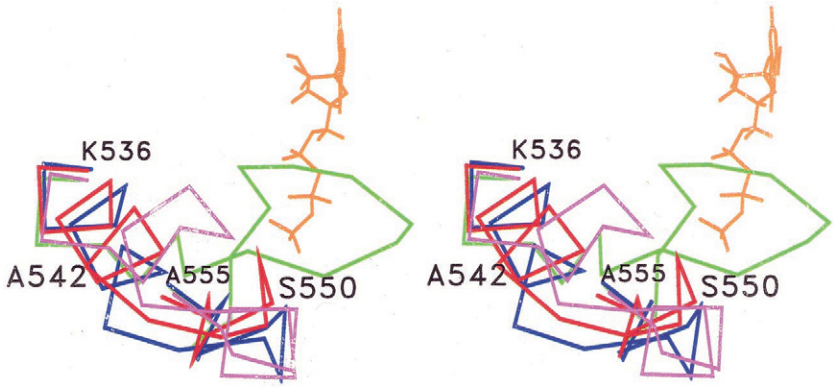

FIGURE 8 Stereo pair of the position of switch 1 (C_α backbone) in the simulated annealing MD in which a closed P_i-tube in the apo-ncd structure was transformed into an open P_i-tube structure. Switch 1 in the initial, closed P_i-tube structure is in green. The conformation after 100 ps of MD at 800 K is shown in blue. The structure after cooling to 300 K is in red. Switch 1 from the ncd crystal structure is colored magenta. All structures were overlaid via their P-loops. For spatial reference only, ATP from the initial closed P_i-tube structure with bound ATP is shown in orange. ATP was not part of the simulation.

fact that there are most certainly multiple local free energy minima for open configurations. Thus, the simulation provides further support for an opening and closing of the P_i-tube in kinesin-family motors.

DISCUSSION

We have used molecular dynamics simulations to model ncd bound to MgADP and MgATP with the switch 1 region both adjacent to, and displaced from, the nucleotide phosphates. This displacement of the switch 1 region resulted in a closed or open conformation, respectively, of a P_i-tube in ncd. Our studies were motivated by the observation that the x-ray structures of kinesin-family motors and myosin S1 show notable structural homology at the nucleotide site, with the sole exception of the location of switch 1. The switch 1 region of S1 was thus used as a guide for closing the ncd P_i-tube. The closing of the P_i-tube required breaking an α-helix (α3a) and repositioning 12 amino acid residues, some by distances greater than 10 Å. Encouragingly, we found that all four nucleotide-bound MD structures in both open- and closed-P_i-tube conformers were stable for the 500 ps of MD, representing local minima on a global free energy landscape. High-temperature dynamics and simulated annealing produced a closed-to-open transition.

Additional confidence in our approach was provided by the close duplication by our modeled, closed structures of the coordination to the nucleotide phosphates, including crystallographic waters, seen in S1 structures. This is not an a priori result, given that the system appears to have a large number of local free energy minima. This is especially true in the case of MgADP. There was mismatch between the nucleotide locations in the superimposed ncd·MgADP structure (taken as the initial location for MgADP) and the S1·MgADP structure. This resulted in a MD simulation in which the MgADP sank ~0.8 Å deeper into a P_i-tube that was bounded by a concurrently deforming switch 1 on one side, before finally establishing protein-ligand coordination very similar to that in the S1·MgADP crystal structure.

We have modeled a closed P_i-tube in kinesin-family motors using ncd as the example. The approach is clearly applicable to other microtubule motors. The choice of ncd was motivated by our observation that if Dd S1 and ncd were superimposed via their respective P-loops, then C_α amino acid atoms at the two ends of the region of interest were in very close spatial proximity. Overlays of kinesin and Kar3 with S1 did not result in such close spatial proximity of amino acids to define the switch 1 region. A comparable modification to the switch 1 region could have been made to these other proteins, but would have then required significantly greater deviations from the crystal structures in the remodeling. Our goal was to remain as true to crystal structures as possible, and thus we chose ncd.

Implications of the MD simulations for ATP hydrolysis by kinesin-family motors

Hydrolysis occurs by an in-line attack on the γ-P_i by a water molecule located at the opposite side of the bridging oxygen-P_γ bond. Due to interaction with the protein, hydrolysis occurs at a rate that is orders of magnitude more rapid than when ATP is free in solution. For the accelerated reaction rate to be attained, the protein must stabilize and optimize the proper spatial relationship between P_γ, the γ-P_i oxygens in the planar transition state intermediate, and the water molecule for the SN2 reaction to occur.

Our present simulations bring into serious question whether this can happen in the open P_i-tube configuration of the ncd crystal structure. Simulations of the open P_i-tube structure with either MgADP or MgATP at the active site indicate that the water constellations formed at the active site are stable on a short time scale, but with waters moving in and out of the constellation on a longer time scale. No specific catalytic water can be identified in either the open or closed P_i-tube MD simulations when MgATP is at the nucleotide site. This is not unexpected because the structure for ATP in our simulations was modeled from a nucleotide triphosphate analog with the γ-P_i oxygens in a tetrahedral

arrangement. However, examination of the final structure from the MgATP simulation with an open P_i-tube identified three representative water molecules located on the opposite side of the bridging oxygen-P_γ bond. The rms deviations from their mean position over the last 200 ps of MD simulation were all in excess of 1 Å. This again emphasizes the significant mobility of the water molecules in the spatial region of interest for catalysis when compared with the benchmark stability of the Pγ (rms deviation < 0.3 Å over the entire 400 ps for all MD simulations with bound nucleotide). In the simulation with the P_i-tube closed, only one water molecule is near the γ-P_i, with a rms deviation in position of only 0.44 Å over the final 300 ps of the simulation. This is less than a 50% difference from P_γ in this simulation, with a rms deviation of 0.29 Å. In Fig. 4, this water is seen to be the one coordinated to Ser 551 and Arg 552 of switch 1 and Thr 436 in the P-loop. The closing of the P_i-tube, and the subsequent ability of switch 1 to interact more directly with the nucleotide, can dramatically enhance the positional stability of not only the nucleotide itself (Table 1), but water as well via elimination of the fluid water constellation. This would appear crucial for hydrolysis, and thus catalytic questions provide another argument in support of our hypothesis of a closing of the P_i-tube during the hydrolysis cycle of kinesin-family motors.

Implications of switch 2 movements

Switch 2 is frequently termed to have an open and closed conformation. This is distinct from, and not to be confused with, the opening and closing of the switch 1 region discussed here. Movements closing switch 2 in motor proteins were first seen in Dd S1 crystal structures when ADP·BeFx was replaced by ADP·AlF^{4-} (Fisher et al., 1995) or ADP·Vi at the active site (Smith and Rayment, 1996b). The opening and closing of switch 2 have been postulated to be an integral part of driving both the myosin power stroke (reviewed in Holmes, 1996; Cooke, 1997) and the kinesin-family motor step (Vale and Milligan, 2000). Comparative movements of switch 2 are demonstrated in the superimposed structures in Fig. 7, where switch 2 is seen to assume three distinct locations. These are labeled *A*, *B*, and *C*. Position *A* is the open switch 2 conformation from the Dd S1·ADP·BeFx structure. It is also the position of switch 2 found in the nucleotide-free, chicken S1 structure and the Dd S1 structures with ADP, AMPPNP, ATPγS, and non-nucleoside diphosphates trapped with BeFx (nine structures total, not shown; see Rayment et al., 1996; Fisher et al., 1995; Gulick et al., 1997, 2000). An extremely surprising observation from our simulations came when the Dd S1·ADP·AlF^{4-} (blue, position *C*) and Dd S1·ADP·Vi (not shown) structures were superimposed via their P-loops on Dm ncd. It was seen that switch 2 from the ATP-closed, final MD structure (red, position *C*) and the S1·ADP·Vi and S1·ADP·AlF^{4-} positions were virtually identical. It is very important to observe that this similarity in position occurs despite dramatically different coordination of switch 2 to the nucleotide, switch 1, and the P-loop in the myosin structure and in the ncd ATP-closed structure from the MD simulation. This can be seen by contrasting our Fig. 4 with Fig. 7 in Fisher et al. (1995) and Fig. 11 in Smith and Rayment (1996a). The location of the switch 2 region in all our other final MD simulations (ATP-open, magenta; ADP-open, gray; ADP-closed, blue) along with the location in the Dd ncd (green), human monomeric kinesin (Kull et al., 1996) (orange), and rat dimeric kinesin crystal structures (Kozielski et al., 1997) (not shown) is in position *B*. The original closing of switch 2 observed in S1 was the blue-to-blue transition from position *A* to position *C*. Relative to *A* and *C*, switch 2 is only half-closed (or half-open) in position *B*. Position *B* is occupied by all kinesin-family motor x-ray structures to date and by all of our simulations, with the sole exception of the ATP-closed, MD simulation. The potential existence of a kinesin-family structure with switch 2 in position *C* implies that current models of kinesin-family motility based upon changes in switch 2 and adjacent structural elements may actually be addressing only one of several intermediate conformations involving switch 2. These models may require revision.

One significant difference in coordination in the open- and closed-switch 2 Dd S1 structures is that the ADP·Vi and ADP·AlF^{4-} structures show a salt bridge between conserved Glu 459 at the C-terminus of switch 2 and Arg 238. The latter is part of the SSR motif in switch 1. The salt bridge is not found in the Dd ADP·BeFx structure. These amino acids correspond to Glu 585 and Arg 552 in ncd, and our ATP-closed MD simulation also does not show a comparable interaction (Fig. 6). Formation of this salt bridge has widely been viewed as an important part of closing switch 2 (reviewed in Vale, 1996, Sack et al., 1999; Vale and Milligan, 2000). Our simulations imply that this may be an overly simplistic interpretation. It is found in some, but not all, x-ray structures from the extended kinesin family MT motors. It is not present in our final ATP-closed structure. Indeed, the ATP-closed simulation shows a completely closed switch 2, but attained via a totally different protein-protein and protein-substrate coordination pattern than has been observed previously in any crystal structure. Thus, the modeling suggests that multiple paths for closing switch 2 probably exist, not necessarily requiring the above salt bridge. Indeed the common feature between all fully closed structures appears to be the hydrogen bond between the switch 2 glycine (G583 in ncd) and a γ-P_i oxygen. In this context, the structure of the smooth muscle S1·ADP·BeFx complex, with a hydrogen bond between the switch 2 glycine and a γ-P_i, tetrahedrally coordinated oxygen, is also in position *C* (orange).

To further investigate the implications of an interaction between Glu 585 and Arg 552, we used the MD result at 500 ps as a starting point and then manually rotated the side

chains Glu 585 and Arg 552, forming a 3-Å salt bridge. An additional 150 ps of MD was then done on the modified structure, and on this time scale, a stable salt bridge was observed. The position of the backbone amino of Gly 583 was basically unaffected, however, displacing only an additional 0.2 Å toward the γ-P_i oxygen. This lack of effect again suggests that the salt bridge simply represents one among multiple possibilities for stabilizing a completely closed switch 2. A single salt bridge provides only modest additional conformational stabilization. The homologous residues in chicken smooth muscle myosin are Glu 470 and Arg 247. The experimental observation that the double mutation E470R, R247E yields a nonfunctional S1 motor in the presence of actin (Onishi et al., 1998) suggests that these residues have a function other than simple formation of a stabilizing salt bridge. This does not contradict the fact that these residues may be crucial for function as the parallel, single mutation experiments of Onishi and co-workers imply.

Relationship to other work

Wriggers and Schulten (1998) have previously used simulated annealing and MD to model conformational changes in the structure of human kinesin containing an open switch 1 region. They did not see a closing of the P_i-tube. Our simulations were done at a higher temperature (300 K vs. 200 K) using a different motor protein, now in both the open and closed conformations. Like Wriggers and Schulten, we did not see a major transition of switch 1. The two sets of simulations also agree in that no change in coordination of switch 2 to the nucleotide is seen when switch 1 is in the open conformation. Wriggers and Schulten included an elastic constraint between the γ-P_i of ATP and Gly 234 (equivalent to the switch 2 Gly 583 in ncd) to study conformational changes in switch 2. The interaction between Gly 583 and the γ-P_i formed naturally in our simulations, but only with ATP at the nucleotide site and the switch 1 region in the closed state. From the opposite perspective, Lawson and co-workers (1997) have used MD to simulate a closed P_i-tube structure, modeling Dd S1 with MgADP·Pi at the nucleotide site. Their simulations also did not show a lateral opening of the P_i-tube. This is despite the fact that experimental data show the P_i-tube in myosin must open sufficiently widely at some point during the hydrolysis cycle in myosin for AP_5A to bind (Pate et al., 1997).

At room temperature, the hydrolysis rates for ncd, kinesin, and S1 are 0.004 s^{-1} (Naber et al., 1997), 0.005 s^{-1} (Ma and Taylor, 1995), and 0.01 s^{-1} (Taylor, 1979), respectively. If we take these values as rough order of magnitude estimates for the frequency of the P_i-tube transition, the inability of any of the MD simulations to detect a P_i-tube conformational change may well be due to the fact that we are looking for an event that is rare on the sub-nanosecond time scale of all of the MD simulations to date. Nonetheless, taken in toto, all the MD simulations clearly indicate thermodynamic stability of both open and closed P_i-tube conformers in motor proteins.

Can movements of switch 1 modulate, or be modulated by, microtubule binding?

We have investigated the implications of an opening and closing of the P_i-tube in MT motors on interactions at the nucleotide site. This is a somewhat myopic perspective as a much larger question remains. Motility appears to require very precise coordination between events occurring at the nucleotide site and at the polymer-binding site. Can motions of the switch 1 region be plausibly related to this coordination? Fig. 9 provides an answer. The C_α backbone of ncd is shown. ADP and the open switch 1 conformation from the x-ray structure are shown. The solvent-exposed loops 7 and 8 are also shown. Cross-linking, proteolysis, and mutation experiments have all implicated L7 and L8 as being part of the MT binding site (Woehlke et al., 1997; Tucker and Goldstein, 1997; Alonso et al., 1998). As seen in Fig. 9, the switch 1 region that would move in opening and closing the P_i-tube is separated from this portion of the MT binding site by only ~20 aa residues, comprised of the surface-exposed protein. One can now posit a very short, structural line of communication between the nucleotide site and the polymer via this pathway. Conformational changes in one could be transmitted to the other, coordinating the alternate binding of polymer and substrate. We also note that in myosin, the larger, upper 50-kDa domain substitutes for the L7-L8 region (topological connectivity is the same) and has also been implicated in the weak binding interaction of myosin with actin. At the L7 N-terminus and switch 1 C-terminus of the region shown in Fig. 9, the communication pathway between the MT binding site and switch 1 is even more direct. Here, the loops are adjacent as they enter the core β-sheet of the protein.

In summary, structural and mechanistic comparisons with other members of the G-protein super-family suggest that the switch 1 region of the microtubule motor, ncd, can exist in both open and closed conformations during the hydrolysis cycle. MD simulations show that both conformations are thermodynamically stable. Furthermore, the MD simulations suggest that the presence of a closed P_i-tube structure in a kinesin-family motor may greatly enhance nucleotide binding, facilitate hydrolysis, and coordinate the nucleotide site with the polymer-binding domain. A closed P_i-tube also appears to be necessary for switch 2 to interact directly with the nucleotide. With MgATP at the active site in the simulations, there is a movement of switch 2 comparable to that observed in myosin crystal structures with ADP·VO_4 and ADP·AlF^{4-} at the active site, but not seen in any kinesin-family motor crystal structure. The latter movement is widely postulated to be a crucial step in the motility cycle. These observations will hopefully spur additional crystallo-

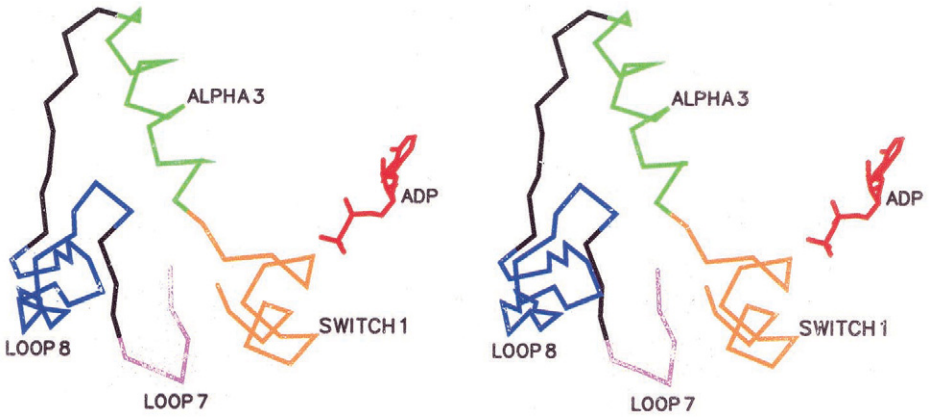

FIGURE 9 Stereo walleye pair showing the close spatial relationship in ncd between the switch 1 region and a portion of the proposed microtubule binding site (L7, magenta; L8, blue) on kinesin-family motors.

graphic efforts to identify open- and closed-conformer motor protein pairs.

Irina Massova is acknowledged for assistance with the free energy calculations. We thank Elena Sablin for providing the coordinates of monomeric ncd before publication and J. David Adcock for help with visualization. The work was supported by U.S. Public Health Service grants AR39643 (E.P.), AR42895 (R.C.), and GM29072 (P.A.K.). T.J.M. was supported by the University of California President's Postdoctoral Fellowship Program. Molecular visualization and structural modifications were done using the UCSF Computer Graphics Laboratory, supported by U.S. Public Health Service grant RR-1081 (T. Ferrin, principal investigator). Computer time was provided by the National Science Foundation supercomputer program at SDSC and NCSA.

REFERENCES

Alonso, M. C., J. van Damme, J. Vandekerckhove, and R. A. Cross. 1998. Proteolytic mapping of kinesin/ncd-microtubule interface: nucleotide dependent conformational changes in loops L8 and L12. *EMBO J.* 17:945–951.

Aqvist, J. 1992. Modelling of ion-ligand interactions in solutions and biomolecules. *J. Mol. Struct. (Theochem.).* 256:135–152.

Bashford, D., D. A. Case, C. Choi, and G. P. Gippert. 1997. Computational study of the role of solvation effects in reverse turn formation in the tetrapeptides APGD and APGN. *J. Am. Chem. Soc.* 119:4964–4971.

Bayly, C. I., P. Cieplak, W. D. Cornell, and P. A. Kollman. 1993. A well-behaved electrostatic potential based method using charge restraints for deriving atomic charges: the RESP model. *J. Phys. Chem.* 97:10269–10280.

Berendsen, H. J. C., J. P. M. Postma, W. F. van Gunsteren, A. DiNola, and J. R. Haak. 1984. Molecular dynamics with coupling to an external bath. *J. Chem. Phys.* 81:3684–3690.

Case, D. A., D. A. Perlman, J. W. Caldwell, T. E. Cheatham III, W. S. Ross, C. L. Simmerling, T. A. Darden, K. M. Merz, R. V. Stanton, A. L. Cheng, J. J. Vincent, M. Crowley, D. M. Ferguson, R. J. Radmer, G. L. Seibel, U. C. Singh, P. K. Weiner, and P. A. Kollman. 1997. AMBER 5, University of California, San Francisco.

Chong, L. T., Y. Duan, L. Wang, I. Massova, and P. A. Kollman. 1999. Molecular dynamics and free-energy calculations applied to affinity maturation in antibody 48G7. *Proc. Natl. Acad. Sci. U.S.A.* 96: 14330–14335.

Cooke, R. 1997. Actomyosin interaction in striated muscle. *Physiol. Rev.* 77:671–691.

Cornell, W. D., P. Cieplak, C. I. Bayly, I. R. Gould, K. M. Merz, D. M. Ferguson, D. C. Spellmeyer, T. Fox, J. W. Caldwell, and P. A. Kollman. 1995. A second generation force field for the simulation of proteins, nucleic acids, and organic molecules. *J. Am. Chem. Soc.* 117: 5179–5197.

Demchuk, E., D. Bashford, G. Gippert, and D. A. Case. 1997. Thermodynamics of a reverse turn motif. Solvent effects and side-chain packing. *J. Mol. Biol.* 270:305–317.

Dominguez, R., Y. Freyzon, K. M. Trybus, and C. Cohen. 1998. Crystal structure of a vertebrate smooth muscle myosin motor domain and its complex with the essential light chain: visualization of the pre-power stroke state. *Cell.* 94:559–571.

Ferrin, T. E., C. C. Huang, L. E. Jarvis, and R. Langridge. 1988. The MIDAS display system. *J. Mol. Graphics.* 6:13–27.

Fisher, A. J., C. A. Smith, J. B. Thoden, R. Smith, K. Sutoh, H. M. Holden, and I. Rayment. 1995. X-ray structures of the myosin motor domain of *Dictyostelium discoideum* complexed with MgADP·BeFx and MgADP·AlF^{4-}. *Biochemistry.* 34:8960–8972.

Goldberg, J. 1999. Structural and functional analysis of the ARF1-ARFGAP complex reveals a role for coatomer in GTP hydrolysis. *Cell.* 96:893–902.

Gulick, A. M., C. B. Bauer, J. B. Thoden, and I. Rayment. 1997. X-ray structures of the MgADP, MgATPγS, and MgAMPPNP complexes of the *Dictyostelium discoideum* myosin motor domain. *Biochemistry.* 36: 11619–11628.

Gulick, A. M., C. B. Bauer, J. B. Thoden, E. Pate, R. G. Yount, and I. Rayment. 2000. X-ray structures of the *Dictyostelium* myosin motor domain with six non-nucleotide analogs. *J. Biol. Chem.* 275:398–408.

Gulick, A. M., H. Song, S. A. Endow, and I. Rayment. 1998. X-ray crystal structure of the yeast Kar3 motor domain complexed with Mg-ADP to 2.3 angstrom resolution. *Biochemistry.* 37:1769–1776.

Holmes, K. C. 1996. Muscle proteins: their actions and interactions. *Curr. Opin. Struct. Biol.* 6:781–789.

Honig, B., K. Sharp, and A. S. Yang. 1993. Macroscopic models of aqueous solutions: biological and chemical applications. *J. Phys. Chem.* 97:1101–1109.

Houdusse, A., V. N. Kalabokis, D. Himmel, A. G. Szent-Gyorgyi, and C. Cohen. 1999. Atomic structure of scallop myosin subfragment S1 complexed with MgADP: a novel conformation of the myosin head. *Cell.* 97:459–470.

Jorgensen, W. L., J. Chandrasekhar, J. D. Madura, R. W. Impey, and M. L. Klein. 1983. Comparison of simple potential functions for simulating liquid water. *J. Comput. Phys.* 79:926–935.

Kjeldgaard, M. K., P. Nissen, S. Thirup, and J. Nyborg. 1993. The crystal structure of elongation factor EF-Tu from *Thermus aquaticus* in the GTP conformation. *Structure.* 1:35–50.

Kozielski, F., S. Sack, A. Marx, M. Thormahlen, E. Schonbrunn, V. Biou, A. Thompson, E. M. Mandelkow, and E. Mandelkow. 1997. The crystal structure of dimeric kinesin and implications for microtubule-dependent motility. *Cell.* 91:985–994.

Kull, F. J., E. P. Sablin, R. Lau, R. J. Fletterick, and R. D. Vale. 1996. Crystal structure of the kinesin motor domain reveals a structural similarity to myosin. *Nature.* 380:550–555.

Kull, F. J., R. D. Vale, and R. J. Fletterick. 1998. The case for a common ancestor: kinesin and myosin motor proteins and G proteins. *J. Muscle Res. Cell Motil.* 19:877–886.

Lawson, J. D., R. G. Yount, and I. Rayment. 1997. Analysis of structural factors influencing "back door" P_i release in myosin. *Biophys. J.* 72: A340.

Ma, Y. Z., and E. W. Taylor. 1995. Kinetic mechanism of kinesin motor domain. *Biochemistry.* 34:13233–13241.

Ma, Y. Z., and E. W. Taylor. 1997. Kinetic mechanism of a monomeric kinesin construct. *J. Biol. Chem.* 272:717–723.

Massova, I., and P. A. Kollman. 1999. Computational alanine scanning to probe protein-protein interactions: a novel approach to evaluate binding free energies. *J. Am. Chem. Soc.* 121:8133–8143.

Minehardt, T., N. Naber, R. Cooke, E. Pate, and P. Kollman. 2000. Simulation of nucleotide binding to myosin. *Biophys. J.* 78:A1455.

Müller, J., A. Marx, S. Sack, Y. H. Song, and E. Mandelkow. 1999. The structure of the nucleotide-binding site of kinesin. *Biol. Chem.* 380: 981–992.

Naber, N., R. Cooke, and E. Pate. 1997. Binding of ncd to microtubules induces a conformational change near the junction of the motor domain with the neck. *Biochemistry.* 36:9681–9689.

Onishi, H., S. Kojima, K. Katoh, K. Fujiwara, H. M. Martinez, and M. F. Morales. 1998. Functional transitions in myosin: formation of a critical salt-bridge and transmission of effect to the sensitive tryptophan. *Proc. Natl. Acad. Sci. U.S.A.* 95:6653–6658.

Osapay, K., W. Young, D. Bashford, C. L. Brooks III, and D. A. Case. 1996. Dielectric continuum models for hydration effects on peptide conformational transitions. *J. Phys. Chem.* 100:2698–2705.

Pai, E. F., U. Krengel, G. A. Petsko, R. S. Goody, W. Kabsch, and A. Wittinghofer. 1990. Refined crystal structure of the triphosphate conformation of H-ras p21 at 1.35 Å resolution: implications for the mechanism of GTP hydrolysis. *EMBO J.* 9:2351–2359.

Pate, E. 1999. Closing of the nucleotide site, Pi-tube in ncd. *Biophys. J.* 76:A45.

Pate, E., N. Naber, M. Matuska, K. Franks-Skiba, and R. Cooke. 1997. Opening of the myosin nucleotide triphosphate binding domain during the ATPase cycle. *Biochemistry.* 36:12155–12166.

Pearlman, D. A., D. A. Case, J. W. Caldwell, W. S. Ross, T. E. Cheatham III, S. DeBolt, D. Ferguson, G. Seibel, and P. A. Kollman. 1995. AMBER, a package of computer programs for applying molecular mechanics, normal mode analysis, molecular dynamics, and free energy calculations to simulate the structural and energetic properties of molecules. *Comp. Phys. Commun.* 91:1–41.

Rayment, I., C. Smith, and R. G. Yount. 1996. The active site of myosin. *Annu. Rev. Phys.* 58:671–702.

Ryckaert, J. P., G. Ciccotti, and H. J. C. Berendsen. 1977. Numerical-integration of cartesian equations of motion of a system with constraints: molecular-dynamics of *n*-alkanes. *J. Comput. Phys.* 23:327–341.

Sablin, E. P., R. B. Case, S. C. Dai, C. L. Hart, A. Ruby, R. D. Vale, and R. J. Fletterick. 1998. Direction determination in the minus-end-directed kinesin motor ncd. *Nature.* 395:813–816.

Sablin, E. P., F. J. Kull, R. Cooke, R. D. Vale, and R. J. Fletterick. 1996. Crystal structure of the motor domain of the kinesin-related motor ncd. *Nature.* 380:555–559.

Sack, S., F. J. Kull, and E. Mandelkow. 1999. Motor proteins of the kinesin family. Structures, variations, and nucleotide binding sites. *Eur. J. Biochem.* 262:1–11.

Sanner, M. F., A. J. Olson, and J. C. Spehner. 1996. Reduced surface: an efficient way to compute molecular species. *Biopolymers.* 38:302–320.

Sharp, K. A., and B. Honig. 1990. Electrostatic interactions in macromolecules: theory and applications. *Annu. Rev. Biophys. Biophys. Chem.* 19:301–332.

Sleep, J., C. Herrmann, T. Barman, and F. Travers. 1994. Inhibition of ATP binding to myofibrils and acto-myosin subfragment 1 by caged ATP. *Biochemistry.* 33:6038–6042.

Smith, K. C., and B. Honig. 1994. Evaluation of the conformational free energies of loops in proteins. *Proteins.* 18:119–132.

Smith, C. A., and I. Rayment. 1996a. X-ray structure of the magnesium(II)-ADP-vanadate complex of the *Dictyostelium discoideum* myosin motor domain to 1.9 angstrom resolution. *Biochemistry.* 35:5404–5417.

Smith, C. A., and I. Rayment. 1996b. Active site comparisons highlight structural similarities between myosin and other P-loop proteins. *Biophys. J.* 70:1590–1602.

Srinivasan, J., T. E. Cheatham III, P. Cieplak, P. A. Kollman, and D. A. Case. 1998. Continuum solvent studies of the stability of DNA, RNA, and phosphoramidate-DNA helices. *J. Am. Chem. Soc.* 120:9401–9409.

Taylor, E. W. 1979. Mechanism of the actomyosin ATPase and the problem of muscle contraction. *Crit. Rev. Biochem.* 7:103–135.

Tong, L., A. M. de Vos, M. V. Milburn, and S-H. Kim. 1991. Crystal structures at 2.2 Å resolution of the catalytic domains of normal ras protein and an oncogenic mutant complexed with GDP. *J. Mol. Biol.* 217:503–516.

Tucker, C., and L. S. B. Goldstein. 1997. Probing the kinesin-microtubule interaction. *J. Biol. Chem.* 272:9481–9488.

Vale, R. D. 1996. Switches, latches, and amplifiers: Common themes of molecular motors. *J. Cell Biol.* 135:291–302.

Vale, R. D., and R. A. Milligan. 2000. The way things move: looking under the hood of molecular motor proteins. *Science.* 288:88–95.

Walker, J. E., M. Saraste, M. J. Runswick, and N. J. Gay. 1982. Distantly related sequences in the a- and b-subunits of ATP synthase, myosin, kinases and other ATP-requiring enzymes and a common nucleotide binding fold. *EMBO J.* 1:945–951.

Woehlke, G., A. K. Ruby, C. L. Hart, B. Ly, N. Hom-Booher, and R. D. Vale. 1997. Microtubule interaction site of the kinesin motor. *Cell.* 90:207–216.

Wriggers, W., and K. Schulten. 1998. Nucleotide-dependent movements of the kinesin motor domain predicted by simulated annealing. *Biophys. J.* 75:646–661.

Yang, A. S., B. Hitz, and B. Honig. 1996. Free energy determinants of secondary structure formation. III. Beta-turns and their role in protein folding. *J. Mol. Biol.* 259:873–882.

Yang, A. S., and B. Honig. 1995a. Free energy determinants of secondary structure formation. I. Alpha-helices. *J. Mol. Biol.* 252:351–365.

Yang, A. S., and B. Honig. 1995b. Free energy determinants of secondary structure formation. II. Antiparallel beta-sheets. *J. Mol. Biol.* 252: 366–376.

Yount, R. G., D. Lawson, and I. Rayment. 1995. Is myosin a "back door" enzyme? *Biophys. J.* 68:44S–47S.